Dynamic Rigorous Modelling of the NO_x Absorption Process: Model Validation with Industrial Data and Process Responses Analyses

Inês L.S.B. Vilarinho,[*,†,§] Belmiro P.M. Duarte,[‡,†] Susana E.F.M. Pereira,[¶] and Nuno M.C. Oliveira[†]

†*CIEPQPF, Department of Chemical Engineering, University of Coimbra, Rua Sílvio Lima, Pólo II, Coimbra 3030–790, Portugal.*

‡*Department of Chemical and Biological Engineering, ISEC, Polytechnic Institute of Coimbra, Rua Pedro Nunes, Quinta da Nora,Coimbra 3030–199, Portugal.*

¶*Bondalti Chemicals, Quinta da Indústria - Rua do Amoníaco Português, 10, Beduído, Estarreja 3860–680, Portugal.*

§*Current address: CICECO–Centre for Research in Ceramics and Composite Materials, University of Aveiro, Aveiro 3810-193, Portugal.*

E-mail: inessvilarinho@ua.pt

Phone: +351 927563434

Abstract

The reduction of NO_x emissions in nitric acid plants during transient regimes still remains a technologically challenging problem. Although these emissions do not violate current environmental regulations, stricter obligations are expected in the near future raising awareness for the need of optimizing NO_x absorption systems. Herein we present a new mathematical model for the dynamics of this process that also simulates

its startup operation. The dynamic mathematical model was implemented in *Mathematica*® and several initialization strategies were required to perform the simulation. The model was validated with industrial data and a throughout analysis was performed to the dynamic process responses during column's startup. We verified that: (i) a reduction of approximately 15 % of the nitric acid lateral stream concentration will lead to a maximum reduction of 6.1 % of the NO_x gas pressures leaving the column, thus reducing the emissions during the startup period; (ii) a decrease of the lateral stream flow rate by 30 % decreases the NO_x peak by 1.30 %; (iii) the increase of the secondary air flow rate did not present significantly influence; (iv) lowering the lateral feed tray two trays below the reference decreases the NO_x emission by 5.9 %. (v) the combined effect of the nitric acid concentration LFT and its position revealed a maximum decrease of 10.0 %. The developed model can also be used to optimize the operational procedures and can be integrated with alternative technologies, like the use of H_2O_2, to further evaluate the NO_x reduction efficiency. Concluding, this tool evidences potential use for dynamic optimization and control and troubleshooting of existing industrial units.

Introduction

Nitric acid production units belong to the class of mature industrial processes. The basic chemistry of its synthesis has not changed in the last hundred years and is composed of essentially three steps[1]:

1. Ammonia combustion that occurs in the ammonia burner:

$$4\,NH_3(g) + 5\,O_2(g) \longrightarrow 4\,NO(g) + 6\,H_2O(g) \tag{R1}$$

2. Nitric oxide oxidation that occurs along the tubes:

$$2\,NO(g) + O_2(g) \longrightarrow 2\,NO_2(g) \tag{R2}$$

3. Absorption of nitrogen dioxide in water that occurs in the absorption column:

$$3\,NO_2(g) + H_2O(l) \longrightarrow 2\,HNO_3(l) + 2\,NO(g) \tag{R3}$$

Modern nitric acid plants include an abatement system, after the absorption column that can be used to significantly reduce the nitrogen oxides emissions. The most used technology

in such systems is the selective catalytic reduction (SCR) that converts the NO_x gases with the aid of a catalyst into N_2 and H_2O in presence of ammonia as a reducing agent. However, during transient regimes these SCR systems cannot be used, since they may lead to the formation of explosive byproducts (ammonia nitrite and nitrate) – resulting in the release the NO_x gases to the atmosphere. The European Union specifies a limit of 75 ppmv for NO_x emissions for new nitric acid plants, according to the Best Available Technique (BAT) Reference Document, BREF, however for about 160 h/year the plant's emission can be higher.[2] In the United States, the limit of the NO_x emissions is approximately 200 ppmv (0.50 pounds of NO_x per ton of 100 percent nitric acid produced) not including the emissions during startup, shutdown and malfunction.[1] Nonetheless, these emissions have a visual impact and may lead to formal complaints by the surrounding populations. Additionally, stricter regulations are expected in a near future, also including the transient periods, demanding alternative approaches to further reduce startup emissions.

Although the improvement of NO_x abatement systems seems the most logical step to reduce the current gas emissions, the "simple" enhancement of the absorption process may also lead to significant NO_x reduction with minimal investment. Therefore, the development of a rigorous model capable of reproducing the steady and dynamic states of absorption units is very appealing, since these models can be used to draw conclusions regarding their NO_x emissions. Dynamic modelling is commonly used to improve and optimize processes. For example, Schneider and Górak developed a dynamic model using the two film theory to simulate a reactive absorption column, describing the reactive absorption of sour gases in a packed column. The model led to a Differential Algebraic Equations (DAE) system formed by 30,000 equations (after discretization) whose results were afterwards validated with experimental data. In 2003, Kenig *et al.* published a review on rigorous modelling of reactive absorption processes. The authors proposed a model, later validated for a set of cases, including the steady state of the NO_x absorption. In this reference, the authors state that rate-based simulations have some relevant computational complexities. Specifically,

this type of models require high computational effort which may lead to numerical errors and, consequently, limit its application to industrial problems. Later, Ref. 6 studied the implementation of rate based models for design and control applications. The authors used the orthogonal collocation on finite elements (OCFE) technique for discretization. The simulation was implemented in gPROMS and the results were validated with experimental data from a NO_x packed column, operating at 600 kPa at steady state and producing a nitric acid concentration of 32 %wt. The dynamic simulation was only used to demonstrate the control system response when increasing NO_x inlet concentrations. Dalaouti and Seferlis have also developed a rate based dynamic model in gPROMS which was validated with NO_x industrial data at steady state. The proposed model predicts the dynamic response to a disturbance with different proportional-integral (PI) controllers. Several numerical tests were reported to guarantee a stable operation while controlling the NO_x emissions. Later, Ref. 8 proposed a unified model approach. This model combined a rigorous non-equilibrium rate based model with order reduction using the OCFE method. For demonstration, the authors studied a NO_x column operating at 560 kPa and producing HNO_3 at 53 %wt.

Our framework uses the industrial absorption column of Bondalti Chemicals as reference which is enclosed in the nitric acid plant and promotes the absorption of nitrous oxides with water. Specific characteristics of this system are: (i) operating pressures between 900 kPa and 1400 kPa; (ii) production of nitric acid at 68 %wt ; (iii) presence of a lateral feed stream with weak nitric acid, approximetely 40 %wt ; and (iv) existence of a cooling system placed inside the absorption unit to promote the release of the heat generated by the reactions. The column's temperature range is between 293.15 K and 323.15 K.

Considering the research work referred above as well as the complexity of the absorption process, we consider that the simulation of the NO_x absorption process, in both the steady and transient regimes, is still challenging. For a model to accurately capture the process dynamics of nitric acid formation and NO_x release, several issues need to be handle. Thus, we propose a rigorous mathematical model which include the following novelties: (i) the

rigorous simulation of absorption units operating near the nitric acid azeotropic conditions, 68 % wt; (ii) the simulation at high pressure operation, nearly 1000 kPa; (iii) the nitrous acid decomposition description; (iv) the consistency of the model at equilibrium conditions; (v) the dynamic simulation of an NO_x absorption column; (vi) an effective comparison of the results with industrial data; and (vii) the simulation of a typical startup. The detailed mathematical model is described in Ref. 9 and in this article we present the dynamic responses of the system, analyses of the most important parameters during the nitric acid plants startup and process responses to disturbances.

Rigorous Rate-based Model

The rate-based dynamic model for the NO_x absorption in water leads to a DAE system whose form is

$$\frac{d\boldsymbol{x}}{dt} = \boldsymbol{x}' = f(\boldsymbol{x}, z, u) \tag{1a}$$

$$0 = g(\boldsymbol{x}, z, u) \tag{1b}$$

where $\boldsymbol{x} \in \mathbb{R}^{n_d}$ stands for the vector of differential state variables, $z \in \mathbb{R}^{n_a}$ for the vector of algebraic variables, $u \in \mathbb{R}^m$ input variables, $\boldsymbol{x}'$ stands for the time derivative of $\boldsymbol{x}$, $f(.) \in \mathbb{R}^{n_v}$ and $g(.) \in \mathbb{R}^{n_v}$ are vectors of functions. An important concept in the analysis of DAEs is the index of the system, commonly used as a measure of the difficulty of the numerical solution. The higher its value, the harder it is to solve the system.[10,11] Although several definitions can be found in the literature, the differentiation index is typically employed. Here, the index of the system is defined as the number of times the algebraic equations of the system must be differentiated in order to obtain a standard form of an ordinary differential equation (ODE) system.[11] In our case, if the Jacobian matrix $\partial g/\partial z$ is non-singular, the system can be converted into a set of ODEs, where the time derivative $z' = dz/dt$ can be obtained from Equation (1b). Thus, the system of Equations (1) is of index-1.[12] Various methods can

be used for the numerical integration of these type of equations such as:[10,13] (i) Backward Differentiation Formulae (BDF) or the Gear method, (ii) Extrapolation methods, and (iii) Implicit Runge-Kutta (Orthogonal Collocation) methods, among others. Another measure of the difficulty of integration a dynamic model is the degree of stiffness. Among the options available, the implicit BDF methods with variable order and step are widely used for this class of problems due to their good stability properties.[14]

The numerical solution of our model is a challenging task due to the scale of the problem, which involves about 25 000 equations, the range of operating conditions where it will be used, which is considerably broad, the high non-linearity and the difference in magnitude achieved by some of the variables. In this study we use the model developed for the NO_x absorption column described in Ref. 9. Note that it has a general structure and can be adapted to simulate different units. Herein, we use the industrial absorption column of Bondalti Chemicals for reference which is enclosed in the nitric acid plant and promotes the absorption of nitrogen oxides with water.

The dynamic model was implemented in *Mathematica*®, and the built-in NDSolve numerical routine was used to integrate the DAE system once it takes advantage of the matrix sparsity, uses symbolic manipulation, uses the high quality IDA solver, that relies on efficient BDF methods, providing numerical solutions with high accuracy and all software components are well maintained. The integration of DAE system requires consistent initial conditions obtained solving the steady state version of the model which requires an algebraic equation solver.

Results

The NO_x absorption column was simulated dynamically in order to evaluate its NO_x reduction capacity during nitric acid plants'startup. All the results presented onwards are displayed in normalized scales to protect the technology licensor and the acid producer. In

all cases the normalization factor used is the maximum value observed.

Dynamic model validation

The dynamic model was validated comparing the simulation results with industrial data. For this purpose, we introduced a ramp disturbance in the column's inlet pressure with a normalized slope of 3.65×10^{-5} s^{-1} and duration of 1440 s, keeping constant values afterwards.

Figure 1 compares the model predictions with gas data collected by on-site monitoring system which measures the NO and NO_x pressures before the abatement reactor, hereby denoted by EnviNO_x®. Note that the model predicts the dynamics of the variables in the stream leaving the column, while the measurements are taken downstream. Although the residence time of the gas in the piping connecting the column to the EnviNO_x® is small (a few seconds), the oxidation reaction of the remaining NO still progresses, and the temperature increases approximately 300 K due to the existing heat exchangers, changing the composition significantly due to gas equilibria. Despite these differences, the simulation results compare fairly well with those collected from the plant. We observe that the model response trend is similar to that measured on-site and the error is below 4.70 % and 3.95 % for the normalized NO pressure, NP_{NO}, and the normalized NO_x pressure, NP_{NO_x}, respectively. Therefore, our dynamic simulation reproduces well the dynamic response of the system and we believe the tool is accurate for simulating the process dynamics.

Column's startup simulation

Typically, there are three different operation steps of the overall startup procedure that contribute for the NO_x emissions: (i) the absorption column filling; (ii) the ignition of the burner with hydrogen; and (iii) the startup of the EnviNO_x® reactor. The NO_x emissions profile during the startup is presented in Figure 2 and two main peaks are observed. The first one is caused by the filling of the absorption column with weak nitric acid, approximately 40 %wt., and has a lower magnitude than the second one. This peak has already been

reduced with relevant modifications in the operating conditions (as observed in the startup II results in Figure 2) and it will not be addressed herein. The second peak is caused by the ignition of the ammonia burner that forms NO_x gases and lasts up to 50 min. The main cause is the inability of using the EnviNO_x® reactor during this period due to safety problems. Consequently, the NO_x gases are not absorbed in the column and are released to the atmosphere.

At the beginning of the column's startup, the inlet gas stream is only formed by air, and a consistent initial solution is required to solve the dynamic model for these conditions. To overcome this problem we simulated the column's steady state with the conditions used at the end of startup and imposed a negative ramp disturbance in the NO_x inlet gas stream composition. In Bondalti Chemicals, the production rate (PR) used at the end of startup corresponds to 70 %. The comparison of plant's data and the model predictions is presented in Figure 3, where the points correspond to the industrial data and the black crosses to the model predictions. Note that the data was retrieved at different plant's relative production rates ranging from 70 % to 80 %. The trays corresponding to smaller normalized values (left side of the graphics and Zone 1) are those located at the bottom of the column, and those with higher normalized values (right side of the graphics and Zone 2) are trays at the top. The lateral feeding stream enters the normalized tray corresponding to 0.5588. Our model does not include enthalpy balances because the cooling system assures that only minor gradients of temperature exist. To explicitly consider the temperature differences across the column we set a temperature profile based on on-site measurements. The used temperature profile is that of the reference plus 1 K (see Ref. 3 for more details):

$$T_n = \begin{cases} 303.66 + 1 & n/N_T > 0.62 \\ 322.63 + 1 - 29.75 n/N_T, & 0.54 \leq n/N_T \leq 0.62 \\ 307.5 + 1 & n/N_T < 0.54 \end{cases} \tag{2}$$

where T_n is the temperature of tray n, N_T the total number of trays and the reference operation corresponds to the steady state conditions attained at PR =95 %. Furthermore, the lateral feed stream enters the same tray used for PR = 95%, the concentration of HNO_3 in the lateral feed stream is 1.5 % above the reference, and the operation pressure in the column is that of the reference minus 170 kPa once these are the conditions obtained for PR = 70%. Observing Figure 3, a reasonably good agreement can be noticed between the nitric acid profile along the column and the model predictions. In Figure 3 we also represented the nitric acid profile at the beginning of startup, blue crosses. In this case we imposed a ramp that reduces the NO_x concentrations until 10 % preventing numerical problems caused by null values during the initialization. Note that the values of the nitric acid concentrations along the column are high due to the lateral feed stream that is composed by weak nitric acid.

The Bondalti's nitric acid startup was analysed and most important operational procedures are presented concomitantly in Figure 4 by splitting the time interval. Different ramps corresponding to feed operations are noted. In Figure 4 the first plot corresponds to the inlet column's pressure, NP_T, the second one to the column's inlet water flowrate, NL_{H_2O}, the third to the secondary air flowrate, $NG_{\text{sec.air}}$ and the last one to the column's outlet NO_x pressures, NP_{NO_x}. Our goal of splitting the time interval is to avoid discontinuities in the mathematical model.

The number of subintervals depends on the number of explicit discontinuities of the system and, in this case, 8 subintervals are specified. In more detail, the sequence of the operations is:

(i) $[t_0, t_1]$ - constant regime;

(ii) $[t_1, t_2]$ - increase the water flow rate;

(iii) $[t_2, t_3]$ - increase the inlet NO_x gas composition, decrease of the total absorption pressure and keep increasing the water flow rate;

(iv) $[t_3, t_4]$ - keep water flow rate constant;

(v) $[t_4, t_5]$ - decrease the inlet water flow rate;

(vi) $[t_3, t_6]$ - increase the total absorption pressure;

(vii) $[t_2, t_7]$ - increase the secundary air flow rate; and

(viii) $[t_7, t_8]$ - stabilize all variables until the steady state is reached.

The observation of NO_x emissions at the beginning of the start up procedure reveals an increase that lasts approximately 860 s. After this increase there are three peaks in the NO_x pressure. Notice that the shape of the peaks is different for every analysed startup, see Ref. 3. We recall that the decrease of the NO_x pressure in the industrial data around 06:30 is caused by the EnviNO$_x$® reactor that was started and represents the end of the nitric acid startup. After this, the plant's production rate is increased to the desired value. From this point forward, there are no major concerns regarding the gas emissions since the NO_x are abated in the EnviNO$_x$® reactor. As a result, the NO_x emissions that the company pretends to reduce are those occurring until 3000 s.

Together with Bondalti Chemicals, we set a reference schedule to simulate the startup of the absorption column, that are mathematical functions describing the inputs profiles captured from Figure 4. The reference was established in order to generate a proper sequence of operations that allows comparing the behaviour of the unit with the model predictions. Practically, we observed a relevant variability in the analysed startup procedures, indicating a certain degree of change in the basic disturbances induced on the unit. A deeper analysis led us to consider that the startup is formed by a sequence of eight stages identified in Figure 4. After this, we characterized each of the ramps forming the overall procedure, and noticed that four input variables change either simultaneously or individually:

- NO_x inlet molar flow rate the sequence is:

(i) increase with a ramp slope of 0.058 s^{-1} (normalized value) from t_1 to t_2; followed by

(ii) a constant value in the interval $[t_2, t_8]$.

- Column's inlet total pressure, we conceptualize the following sequence:

(i) decrease with a normalized ramp slope of 1.05×10^{-4} s^{-1} from t_2 to t_3;

(ii) increase with a normalized ramp slope of 6.73×10^{-5} s^{-1} from t_3 to t_6; followed by

(iii) a period where the value is kept constant, in the interval $[t_6, t_8]$.

- Column's inlet water flow rate, the sequence includes the:

(i) increase with a normalized ramp slope of 0.023 s^{-1} from t_0 to t_1;

(ii) a constant value in the interval $[t_1, t_4]$;

(iii) decrease with a normalized ramp slope of 0.012 s^{-1} from t_4 to t_5; and

(iv) a constant value in the interval $[t_5, t_8]$.

- Secundary air flow rate, the sequence is as follows:

(i) increase with a normalized ramp slope of 6.3×10^{-6} s^{-1} from t_2 to t_7; and

(ii) a constant value in the interval $[t_7, t_8]$.

Figure 5 shows the graphical representation of each modelled ramp.

The NO_x gas pressure leaving the column during the reference startup is presented in Figure 6 together with the industrial data from one startup, where the red line represents the beginning of the abatement reactor and consequently, the NO_x pressures start to decrease. Figure 6 shows some differences between the simulation for the reference case and the industrial data, although a similar overall trend is observed. Note that at the beginning of the start-up (0 seconds) the NO_x pressures leaving the column are not null, because we

already have the influence of the lateral feed stream which cause the release of gas due to desorption. Furthermore, the observed differences between the industrial data and the model may be due to: (i) the denitrification of the absorption column after starting the lateral feed stream. After the absorption column is filled, air passes through the column until the ignition of the burner occurs, and this will cause the denitrification of the liquid phase. This means that the industrial nitric acid profile at the beginning of this startup (orange points in Figure 3) is lower than the one used for simulation (blue line in Figure 3); (ii) the different location of the NO_x pressures sampling points used for comparison (the model simulates the NO_x pressure leaving the absorption column, while on site the data was gathered after the EnviNO_x® reactor); (iii) the assumption that the start-up occurs in the conditions that corresponds to plant's relative production rate of 70 %; and (iv) the inlet gas concentrations at the beginning of the startup that is assumed to be 10 % of that at the steady state conditions for PR=70 %. Nevertheless the NO_x pressure increases at the beginning of the startup and this ramp lasts for approximately 780 s, very close to that observed from industrial data. After the peak in the model predictions, the NO_x pressure decreases until a new steady state is reached. Note that this decrease coincides with the pressure increase, which has a major impact on the system. The other peaks in the industrial data are not observed in the model prediction because the shape of the peak is different in every startup and only the main disturbances were simulated. However, process responses to disturbances can be analysed in order to study and optimize the process procedures in order to reduce the NO_x emissions.

Process responses analyses

The basic goal of using the dynamic model is to forecast the process behaviour when disturbances occur and gather knowledge that can help to improve the process control and the reduction of NO_x peaks during startup. For this purpose we considered the following variables: (i) nitric acid concentration of the lateral feed stream; (ii) flowrate of the lateral feed stream; (iii) secondary air flowrate; and (iv) lateral feed tray position.

The nitric acid concentration of the lateral stream has a strong impact on the profiles within the column, and the lower its concentration the lower the NO_x gas pressure leaving the column.[3] Consequently, we analyse the transient response of the system to a disturbance in this variable. Figure 7 compares the NO_x gas pressure leaving the column during the startup for the reference case, where a lateral feed stream with nitric acid mass fraction of 0.41 (reference) is used, and for a scenario where the lateral nitric acid mass fraction is 0.35.

We observe that the reduction of the lateral stream nitric acid concentration will reduce the NO_x gas concentrations leaving the column. The peak is reduced by approximately 3.9 %, and this decrease is extended to the whole time horizon of the simulation being approximately 6.1 %, at the end. The decrease of the NO_x gas pressures leaving the column is expected since the decrease of the nitric acid concentration in the lateral feed stream will lead to an increase of the NO_x absorption driving force in Zone 1. Due to safety limitations the nitric acid mass fraction cannot be lower than 0.3 below the lateral feed tray consequently, the nitric acid profile along the column at the beginning of the startup operation and after 3000 s is presented, see Figure 8. Here, we observed that at the end of the startup the nitric acid mass fraction in the LFT (corresponding to a normalized tray of 0.56) is lower than 0.3 being 0.286. This value can be tolerated but lower nitric acid mass fractions cannot be used. The nitric acid concentration in the first tray is not relevant during the startup procedure but we can see that it has increased, as expected, from 0.425 to 0.600.

The effects of the lateral feed stream flow rate and secondary air flow rate during the column's startup are herein presented. Figure 9 represents the simulation results for the reference scenario and for a scenario where the flow rate is reduced by 30 %. The analysis of Figure 9 reveals that no considerable impact occurs when reducing the lateral feed stream flow rate by 30 %; specifically, a decrease of 1.3 % is observed at the peak. Figure 10 presents the nitric acid mass fraction profile at the beginning and end of startup. Observing the figure, we can conclude that decreasing the lateral feed stream flow rate will lead to an increase in the absorption rate in Zone 1, compared to the reference case, and consequently,

the HNO_3 concentration is lower in the lateral feed tray. However this reduction is not significant and in Zone 2 the nitric acid profile is similar to that of the reference. Thus, low impact is observed in the NO_x gas stream leaving the column.

The impact of the secondary air flow rate was also analysed, by simulating an increase of 33.3 % with a normalized ramp slope of 1.6×10^{-5} s^{-1}, from t_2 until t_7, as opposed to the reference scenario where an increase of 13.4 % with a normalized ramp slope of 6.3×10^{-6} s^{-1} was used. After the ramp, the secondary air flow rate was kept constant for the remaining period. The comparison of the NO_x gas leaving the column between the reference case and this new scenario is shown in Figure 11. The dynamics do not show significant differences in the NO_x gas concentration leaving the column during the startup. The secondary air flow rate has an impact in the NO oxidation rate as it increases the oxygen content in the inlet gas stream. This increase induces a higher oxidation rate which promotes the increase of the NO_x absorption rate, verified in Figure 12 where the beginning and end of startup profiles are analysed.

Figure 12 shows the influence of increasing the secondary air flow rate along the column and, in this case, no difference is observed when compared to the reference. Consequently, the increase of the secondary air does not have a significant impact on the NO_x pressures leaving the absorption column. Notice that, in this case, the mass fraction in Zone 1 is above 0.3 not causing any safety problems.

Further, the lateral feed tray position was also analysed and the results are presented in Figure 13. Here, a decrease of 3.4 % is observed at the peak and 2.9 % at the end of the startup for one tray and 5.9 % and 5.2 %, respectively when moved the LFT two trays below. Lowering the lateral feed position will increase the reaction volume in Zone 2 (rectifying zone) where the NO_x gases that were not absorbed in Zone 1 can be further absorbed, which was verified my the mathematical model.

Finally, the combined effect of the nitric acid concentration at 0.35 in the LFT and its position, two trays below the reference, was studied and the total NO_x reduction is presented

in the graphical figure. In this case, a decrease of 8.7 % is observed at the peak and 10.0 % at the end of the startup. Moreover, the simulation reveals that the effect of the disturbances on NO_x pressures is additive and both modification can be implemented simultaneously.

In summary, we present a new rigorous rate based model for the NO_x absorption process that analyse the dynamics of an absorption column and simulates a startup operation. From the model results we observed that the nitric acid plant in Bondalti Chemicals can reduce the NO_x emissions implementing some of the disturbances analysed. Furthermore, the mathematical tool presented in this work might be used to study different approaches like the use of H_2O_2 in the absorption column and can also be applied to other units. Concluding, the NO_x emissions in nitric acid plants during transient regimes can be reduced by optimizing plant's startup procedures.

Acknowledgement

The authors thank the financial support by Fundação para a Ciência e Tecnologia (FCT) for the Ph.D. Grant SFRH/BDE/51755/2011 and by Bondalti Chemicals.

References

(1) EPA, U. S. E. P. A. https://www3.epa.gov/ttnchie1/ap42/ch08/bgdocs/b08s08.pdf Accessed Online: September 2018. 2012.

(2) Groves, M.; Frank, C. EnviNOx ® : Process for N2O and NOX Abatement in Nitric Acid Plants Setting emission standards for nitric acid plants. 2009.

(3) Vilarinho, I. Abatement of NO_x emissions in nitric acid plants during transient regimes. Ph.D. thesis, University of Coimbra, 2019.

(4) Schneider, R.; Górak, A. *Chemical Engineering and Technology* **2001**, *24*, 979–989.

(5) Kenig, E. Y.; Kucka, L.; Gorak, A. *Chemical Engineering and Technology* **2003**, *26*, 631–646.

(6) Kenig, E.; Seferlis, P. *Chemical Engineering Progress* **2009**, *105*, 65–73.

(7) Dalaouti, N.; Seferlis, P. *Journal of Cleaner Production* **2005**, *13*, 1461–1470.

(8) Dalaouti, N.; Seferlis, P. *Computers & Chemical Engineering* **2006**, *30*, 1264–1277.

(9) Vilarinho, I. L.; Oliveira, N. M.; Duarte, B. P.; Susana, E. P. *Computer Aided Chemical Engineering* **2016**, *38*, 1479–1484.

(10) Blajer, W. *Applied Mathematical Modelling* **1992**, *16*, 70–77.

(11) Jüttner, K.; Galla, U.; Schmieder, H. *Electrochimica Acta* **2000**, *45*, 2575–2594.

(12) Brenan, K. E.; Campbell, S. L. V.; Petzold, L. R. *Numerical solution of Initial-Value Problems in Differential-Algebraic Equations*; Society for Industrial and Applied Mathematics, 1996.

(13) Vilarinho, I. L.; Oliveira, N. M.; Duarte, B. P.; Susana, E. P. *Chempor2018 13th International Chemical and Biological Engineering Conference* **2018**,

(14) Celaya, E. A.; Aguirrezabala, J. J. A.; Chatzipantelidis, P. Implementation of an adaptive BDF2 formula and comparison with the MATLAB Ode15s. Procedia Computer Science. 2014; pp 1014–1026.

Graphical TOC Entry

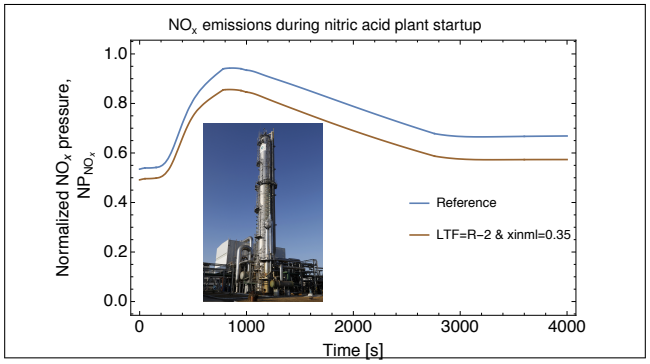

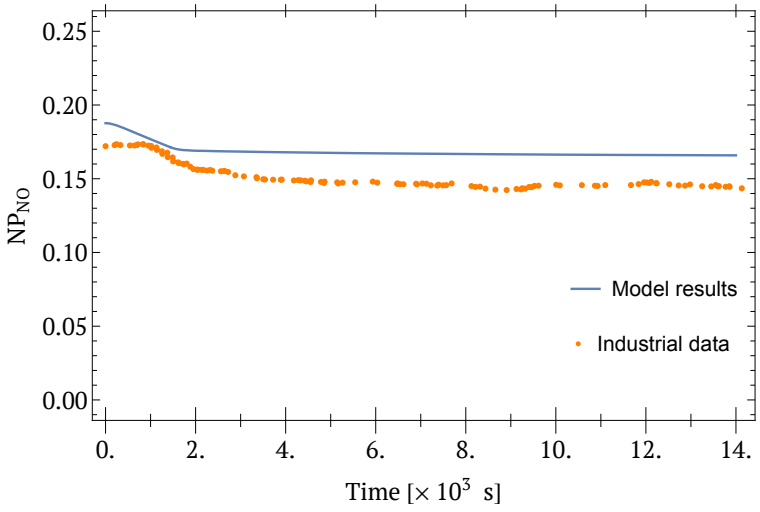

(a) NO in top tray

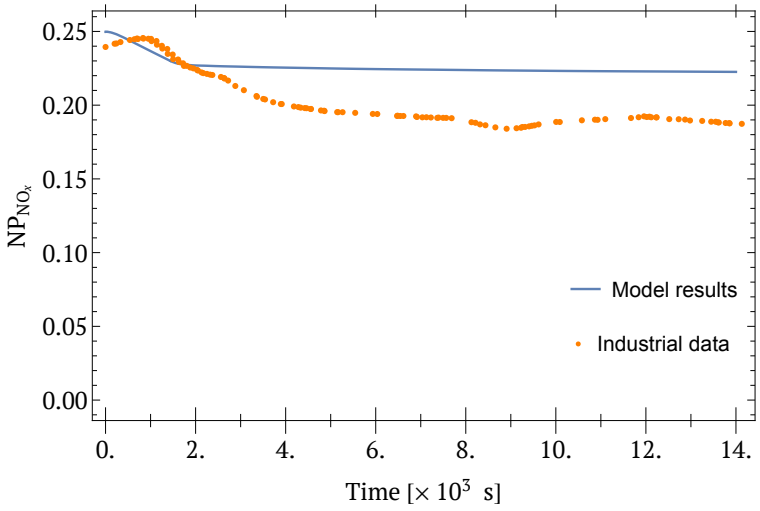

(b) NO_x in top tray

Figure 1: Responses of the leaving gas stream to an inlet pressure ramp disturbance for: (a) Normalized NO pressure;[13] and (b) Normalized NO_x pressure.

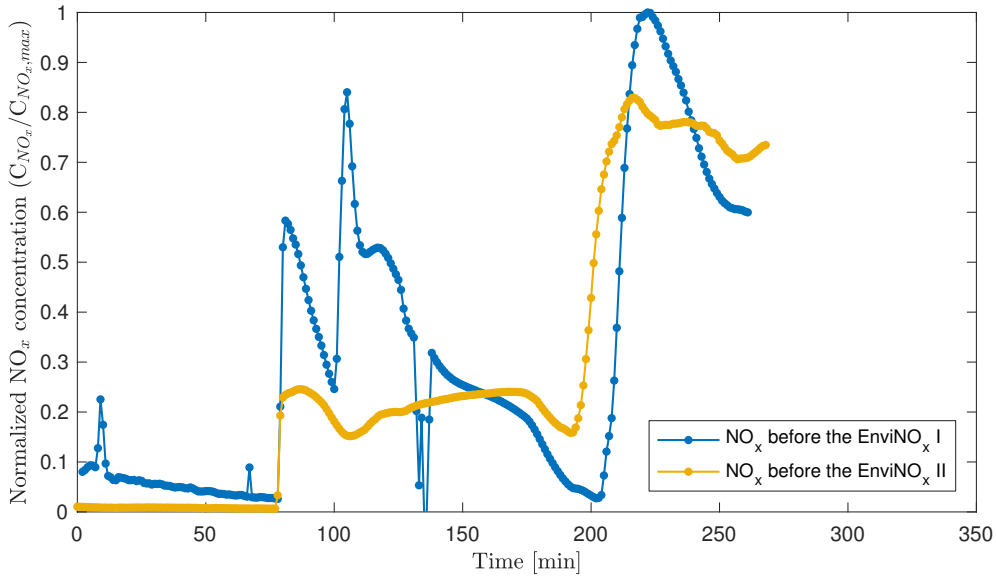

Figure 2: Emissions data (before the EnviNO$_x$®) for two different start-ups operations.

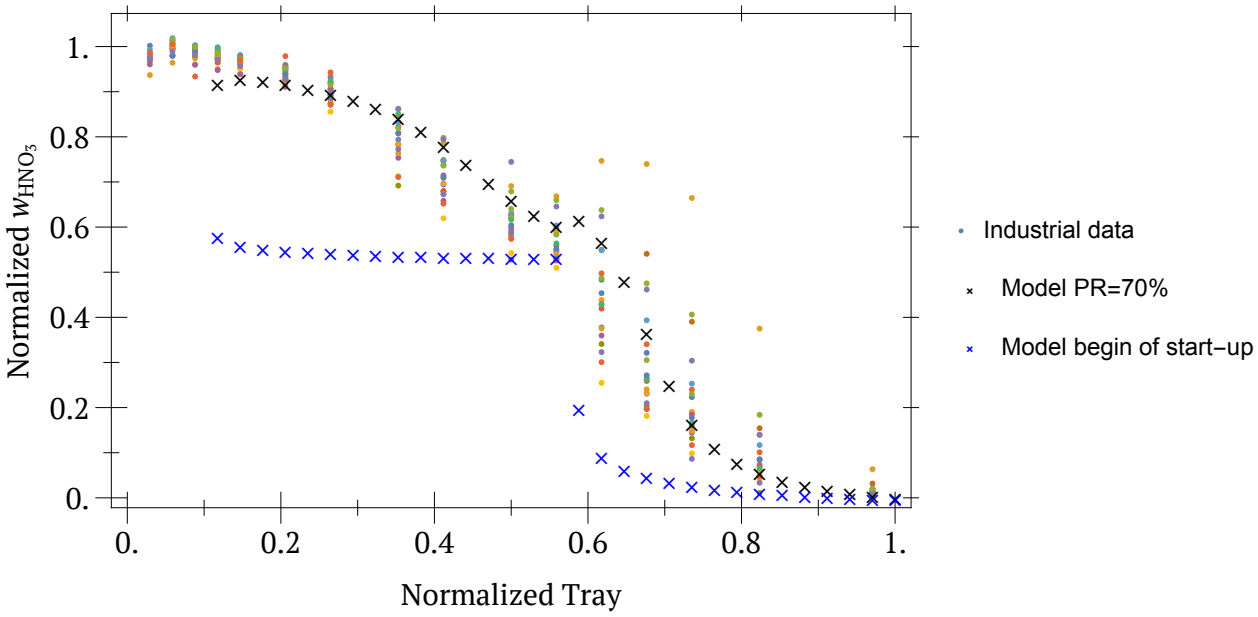

Figure 3: Comparison between plant's data and model predictions for PR =70 %, at the beginning and end of startup.

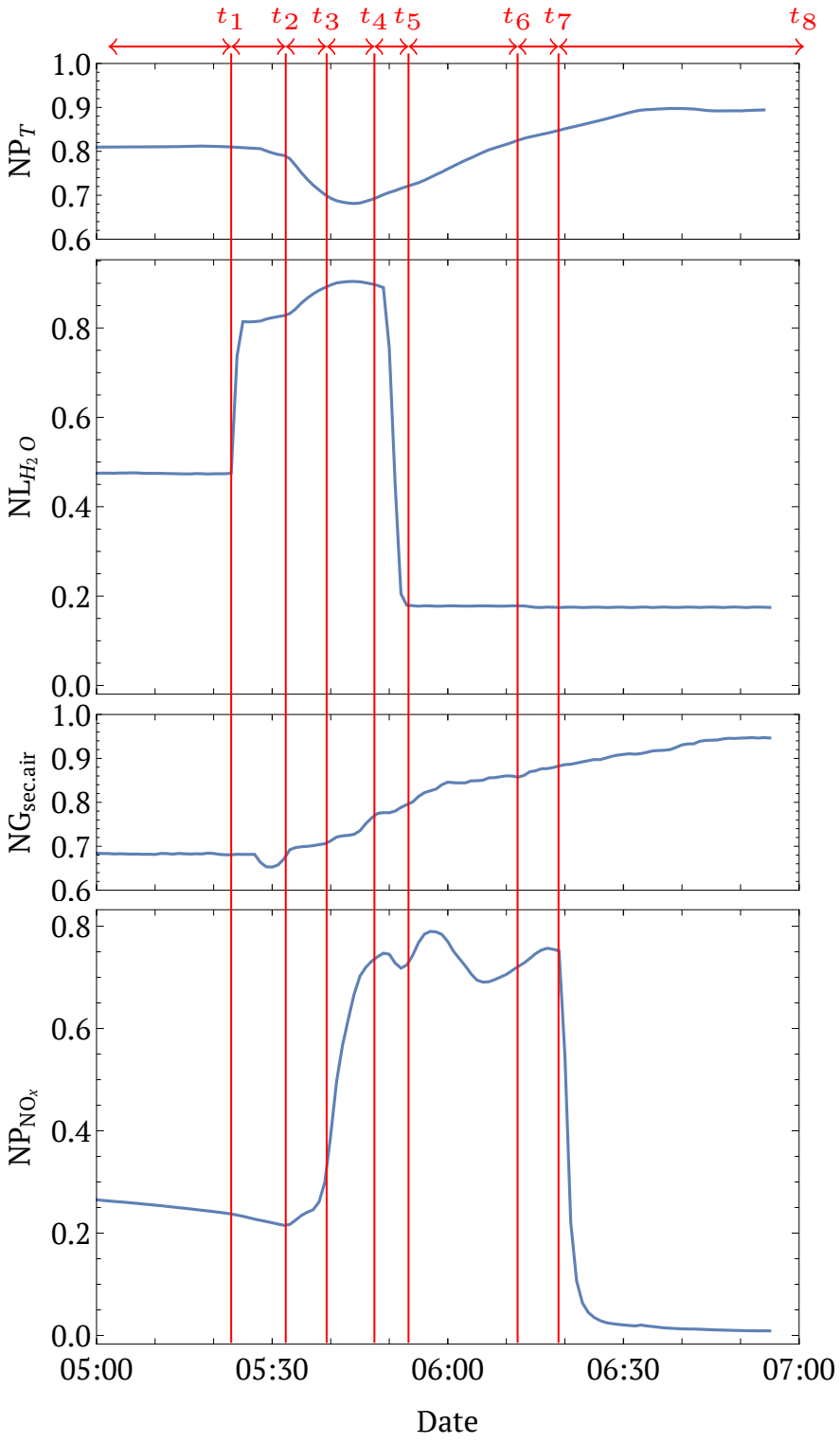

Figure 4: Sequence of the most relevant changes during one startup operation.

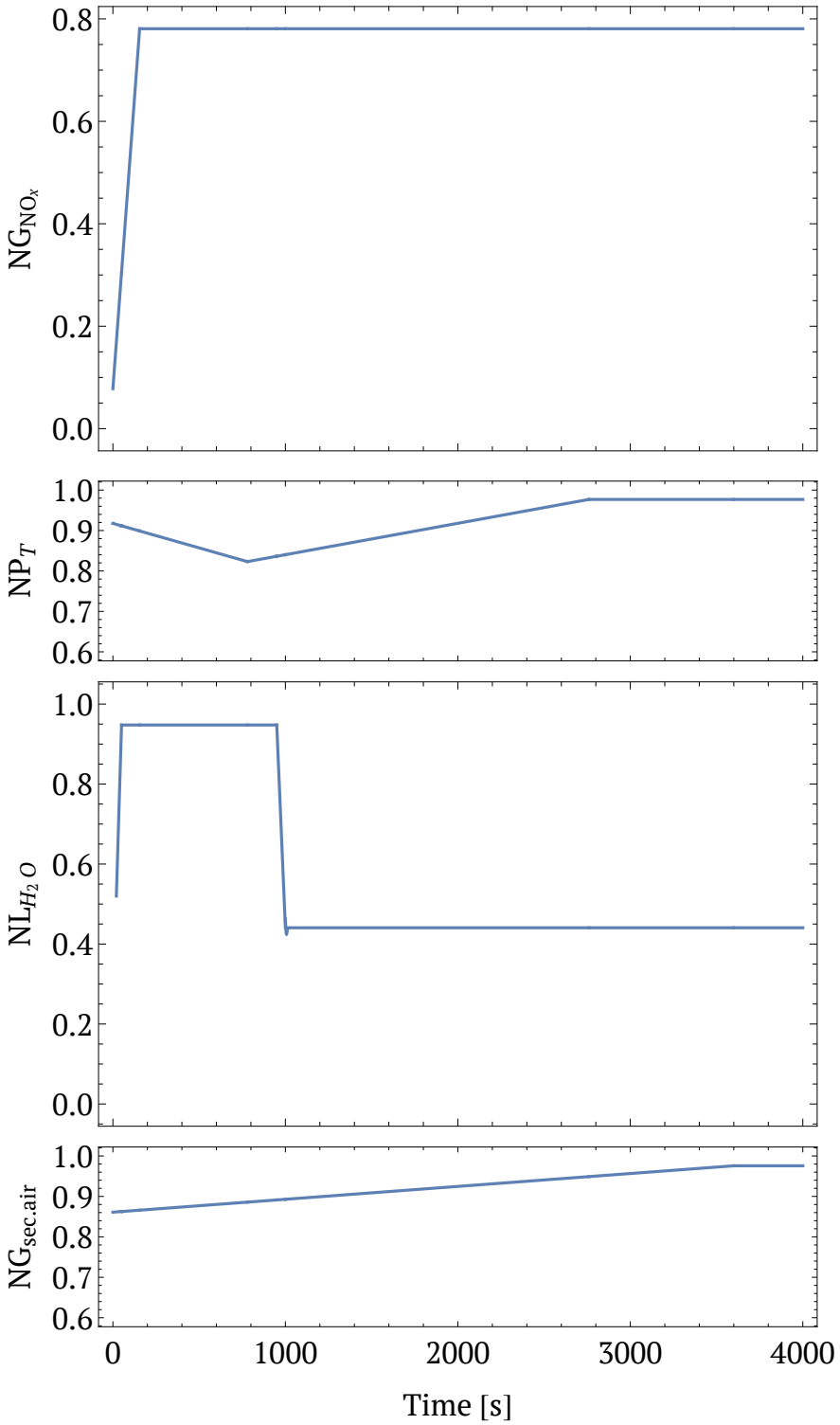

Figure 5: Sequence of ramps of the start-up procedure: the first plot corresponds to the column's inlet NO_x gas flowrate, NG_{NO_x}, the second to the inlet column's pressure, NP_T, the third to the column's inlet water flowrate, NL_{H_2O}, and the last one to the secondary air flowrate, $NG_{sec.air}$.

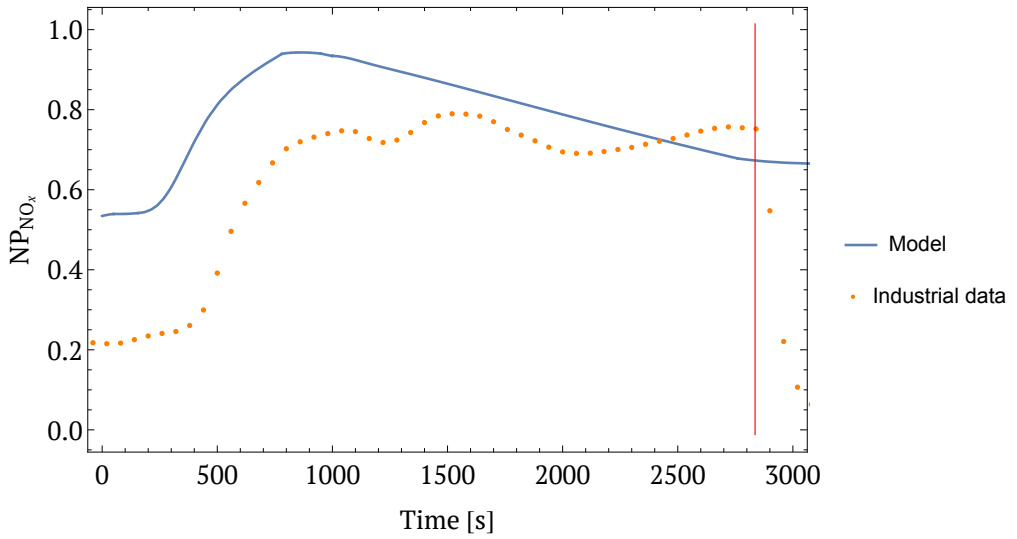

Figure 6: NO_x gas pressure leaving the column during the start-up for the reference case and Start-up I.

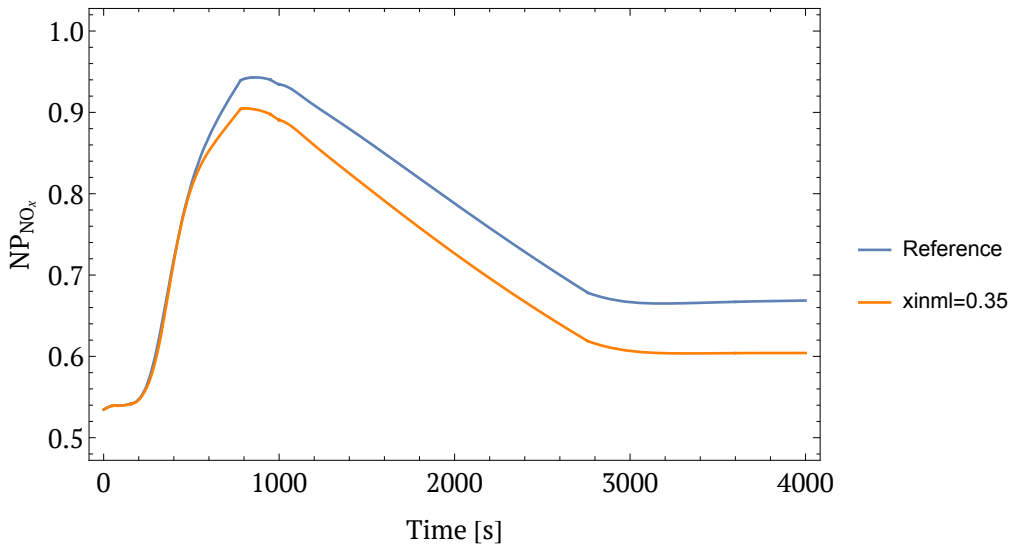

Figure 7: Comparison of the NO_x gas pressure leaving the column between the reference case and when the lateral feed stream nitric acid mass fraction is 0.35.

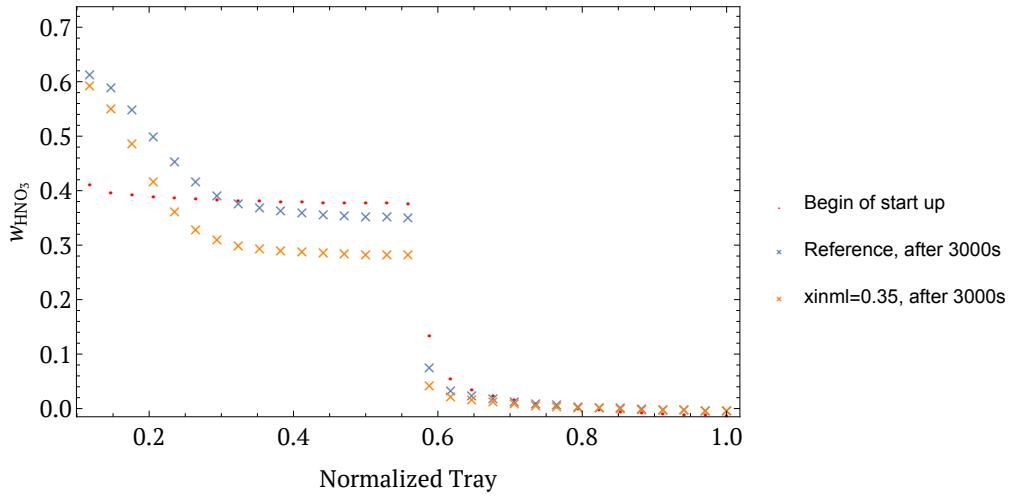

Figure 8: Nitric acid mass fraction profile in the absorption column at the beginning and end of the startup when lateral stream nitric acid mass fraction is reduced.

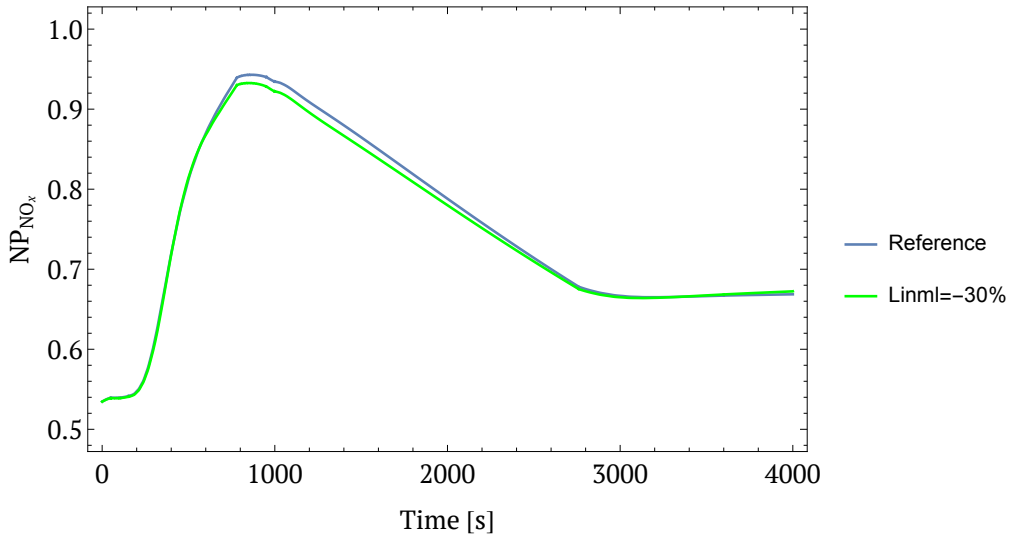

Figure 9: Comparison of the NO_x gas pressure leaving the column between the reference case and in case the lateral feed stream flow rate is reduced by 30 %.

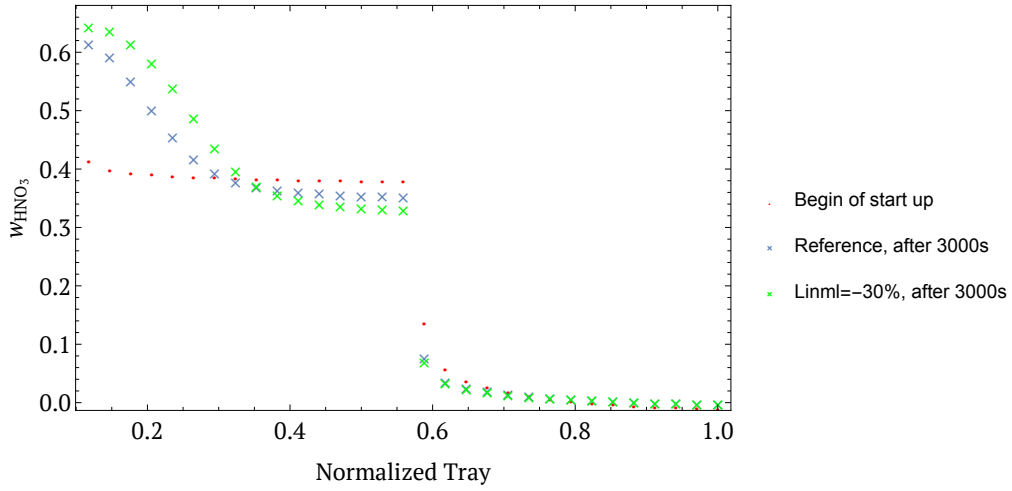

Figure 10: Nitric acid mass fraction profile in the beginning and end of startup in case the lateral stream flow rate is reduced by 30 %.

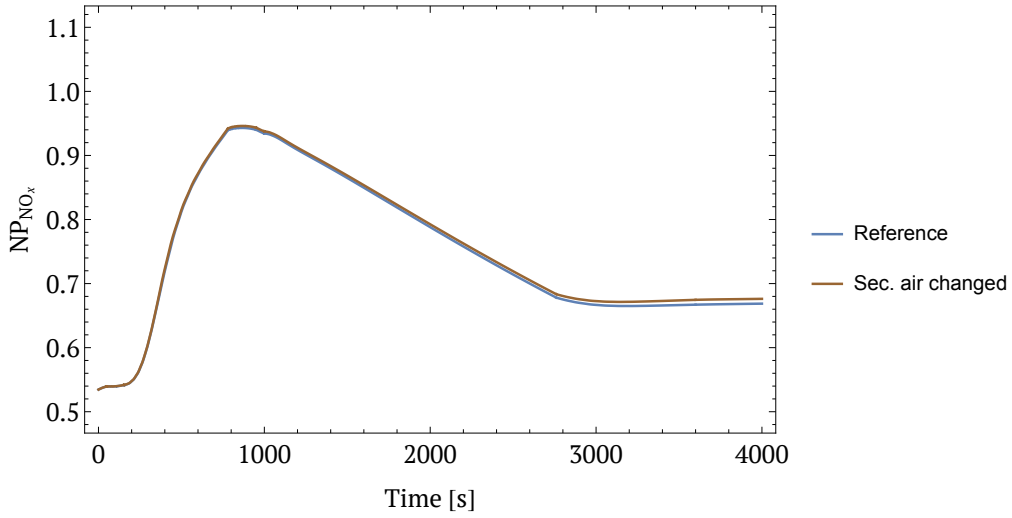

Figure 11: Comparison of the NO_x gas pressure leaving the column between the reference case and in case the secondary air has a different ramp profile.

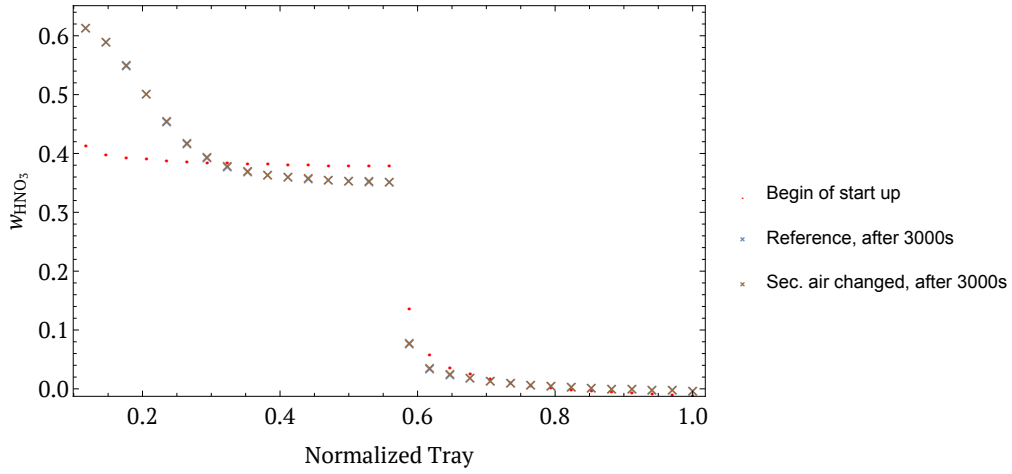

Figure 12: Nitric acid mass fraction profile in the absorption column at the beginning and end of startup in case the secondary air has a different ramp profile.

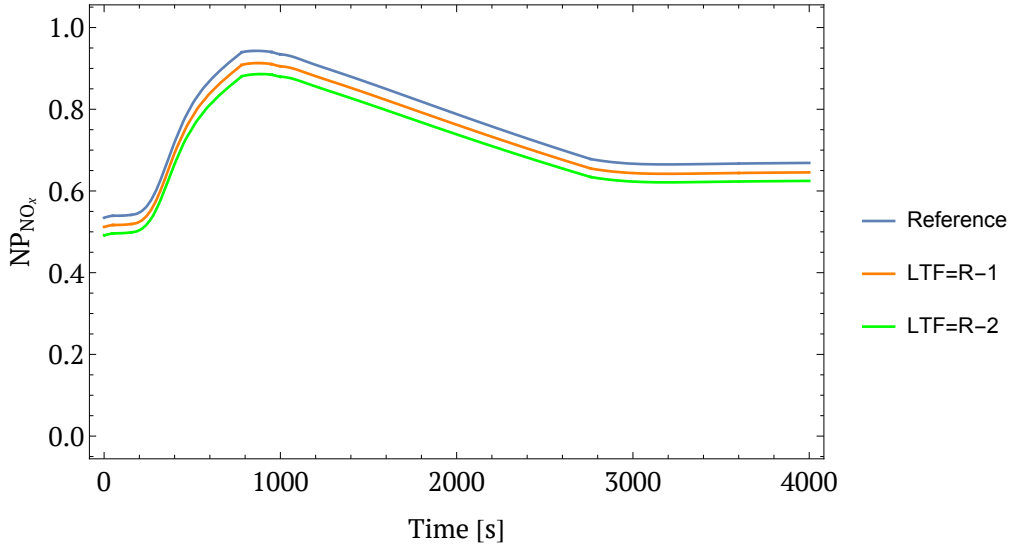

Figure 13: Comparison of the NO_x gas pressure leaving the column between the reference case and when the lateral feed tray is moved 1 and 2 trays below.